

Ben Hui Wang · Ji De Wang · Rui Quan Liu
Ya Hong Xie · Zhi Jie Li

Synthesis of ammonia from natural gas at atmospheric pressure with doped ceria– $\text{Ca}_3(\text{PO}_4)_2$ – K_3PO_4 composite electrolyte and its proton conductivity at intermediate temperature

Received: 3 May 2005 / Revised: 19 May 2005 / Accepted: 7 July 2005 / Published online: 29 September 2005
© Springer-Verlag 2005

Abstract A new type of oxide–salt composite electrolyte, yttrium doped ceria $\text{YDC}-\text{Ca}_3(\text{PO}_4)_2-\text{K}_3\text{PO}_4$, was developed and demonstrated for its promising use for ammonia synthesis. Using this composite electrolyte, ammonia was synthesized from nitrogen and natural gas at atmospheric pressure in the solid-state proton conducting cell reactor, and the optimal condition for ammonia production was determined. The evolved rate of ammonia is up to $6.95 \times 10^{-9} \text{ mol s}^{-1} \text{ cm}^{-2}$.

Keywords $\text{YDC}-\text{Ca}_3(\text{PO}_4)_2-\text{K}_3\text{PO}_4$ · Composite electrolyte · Ammonia synthesis · Natural gas

Introduction

In recent years, various ceria–salt composites as the electrolytes for intermediate temperature solid oxide fuel cells (ITSOFCs, 400–800 °C) have been reported [1–5]. These ceria–salt composites, on one hand, could effectively suppress electronic conduction and enhance the material stability and on the other hand, could demonstrate very high ionic conductivity. These materials are of special interest because of their potential applications as electrolytes in solid oxide fuel cells, hydrogen sensors and synthesis of ammonia electrochemically at intermediate temperature.

Ammonia synthesis from nitrogen and hydrogen, at atmospheric pressure using solid-state proton conductors as the electrolytes, has been investigated in electrochemistry [6–11]. However, there are many problems associated with using H_2 as the source: (1) Most H_2 is

produced from fossil fuels and there is a significant penalty in overall efficiency of the process due to the reforming steps; (2) H_2 is difficult to store; and (3) H_2 is potentially dangerous and requires special safety considerations. Previously, direct use of natural gas in fuel cells has been reported [12]. Although the chemical composition of natural gas varies according to the source, the principal component is methane. Recently, the electrochemical conversion of methane has been given more and more attention [13–15]. However, synthesis of ammonia with the use of solid-state proton conductors from natural gas and nitrogen has not been reported. In this paper, we have developed a new doped ceria– $\text{Ca}_3(\text{PO}_4)_2-\text{K}_3\text{PO}_4$ composite electrolyte, using this composite electrolyte, ammonia was synthesized from natural gas and nitrogen at atmospheric pressure in the solid-state proton conducting cell reactor. The research breakthrough in ammonia synthesis from natural gas has important significance, because natural gas can offer many advantages in comparison to hydrogen. For example, it is relatively abundant and widely available around the world. The optimal condition for ammonia production was determined. The rate of evolution of ammonia is up to $6.95 \times 10^{-9} \text{ mol s}^{-1} \text{ cm}^{-2}$.

Preparation and characterization

$\text{YDC}-\text{Ca}_3(\text{PO}_4)_2-\text{K}_3\text{PO}_4$ composite

Step 1. Nano-structured ion doped ceria, yttrium doped ceria (YDC, $\text{Ce}_{0.8}\text{Y}_{0.2}\text{O}_{1.9}$) was prepared through sol–gel method. Rare earth oxide Y_2O_3 (analytical reagent) in stoichiometric amount was first converted into its nitrate by dissolving in concentrated nitric acid. Calculated amount of $(\text{NH}_4)_2\text{Ce}(\text{NO}_3)_6$ (A.R.) aqueous solution was added to the nitrate solution. Subsequently, solid citric acid was added to the solution, resulting in a mole ratio of citric acid: metal = 2:1. The solution was then slowly evaporated on a water bath until a viscous liquid was obtained. This sol was placed in a

B. H. Wang · J. D. Wang · R. Q. Liu (✉)
Y. H. Xie · Zhi Jie Li
College of Chemistry & Chemical Engineering,
XinJiang University, Urumqi
830046, People Republic of China
E-mail: liu.rq@163.com
Tel.: +86-991-8582807
Fax: +86-991-8582807

constant-temperature drying oven till a solid mass was obtained. Afterwards, the solid mass was calcined in an electric oven for 5 h to form ultra-fine powders. The calcined powders were ground completely for use.

Step 2. Yttrium doped ceria and $\text{Ca}_3(\text{PO}_4)_2$, K_3PO_4 powders were prepared by mixing the YDC and phosphates according to the weight ratio of 80 wt% YDC: 20 wt% binary phosphates. A composition of binary phosphates was used 60 wt% $\text{Ca}_3(\text{PO}_4)_2$: 40 wt% K_3PO_4 . The mixtures of the YDC and binary phosphates were ground and pressed into pellets with about 30 MPa, then sintered in air at 1,400 °C for 10 h to prepare ceramic samples.

Characterization

The morphology was observed by scanning electron microscopy (SEM) and transmission electron microscopy (TEM). A single fluorite-type phase was confirmed by X-ray diffraction (XRD).

Application of the ceramic as electrolyte in the synthesis of ammonia at atmospheric pressure

The equipment used in this study (Fig. 1) and the experimental conditions were described in Ref. [9]. Ammonia was synthesized in the outlet gas using the cell:

natural gas, $\text{Ag} - \text{Pd} | \text{sample} | \text{Ag} - \text{Pd}, \text{N}_2$

NH_3 was adsorbed by 10 ml of dilute sulfuric acid with an initial pH of 3.48. In addition, the concentration of NH_4^+ in the absorption solution was analyzed by using the Nessler's reagent and spectrophotometry [16].

Results and discussion

The analysis of XRD pattern

Figure 2 shows the X-ray diffraction pattern of the composite electrolyte $\text{YDC}-\text{Ca}_3(\text{PO}_4)_2-\text{K}_3\text{PO}_4$. For

Fig. 1 Diagram of the equipment for ammonia synthesis

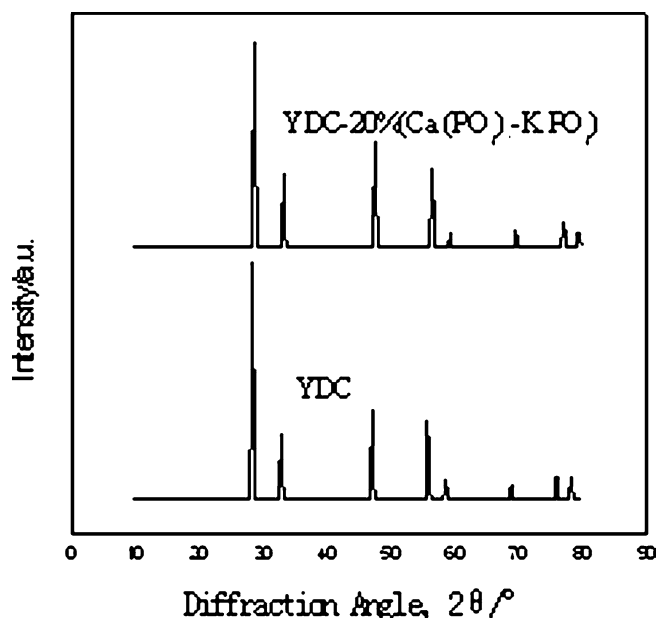
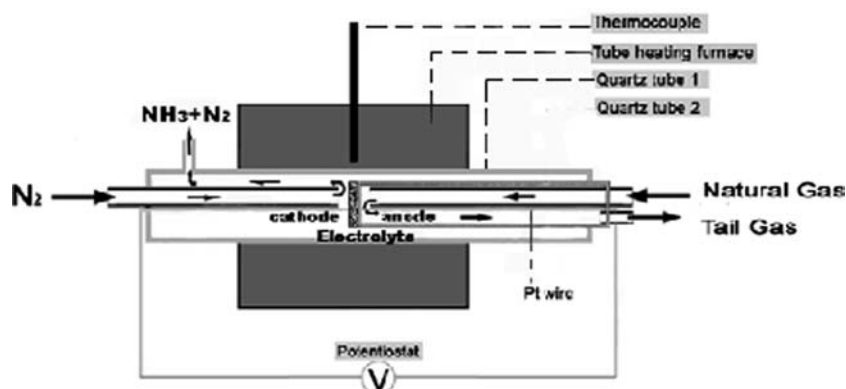


Fig. 2 XRD Patterns of YDC and $\text{YDC}-\text{Ca}_3(\text{PO}_4)_2-\text{K}_3\text{PO}_4$ at 1,400 °C

comparison, the XRD pattern of a single YDC sample was also shown. It can be seen that no peak for crystalline salt phase appears in this pattern, which means the introduction of the phosphates does not change the YDC phase structure. In this case, the $\text{Ca}_3(\text{PO}_4)_2-\text{K}_3\text{PO}_4$ may be assumed to exist as an amorphous phase co-existing with the YDC and very likely to cover on the YDC particles because during the heat treatment the $\text{Ca}_3(\text{PO}_4)_2-\text{K}_3\text{PO}_4$ can be melted and coated on the YDC particles. On the other hand, there are no new XRD patterns observed for the $\text{YDC}-\text{Ca}_3(\text{PO}_4)_2-\text{K}_3\text{PO}_4$, which means there is neither a chemical reaction nor any intermediate compound between the YDC and the $\text{Ca}_3(\text{PO}_4)_2-\text{K}_3\text{PO}_4$ materials/phases [2, 5].

SEM and TEM analyses

Figure 3 shows the TEM image of the YDC powders calcined at 600 °C for 5 h. The average particle size was

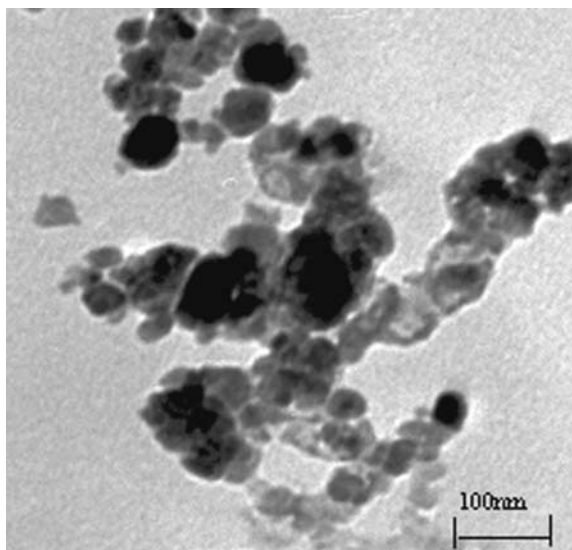


Fig. 3 TEM image of $\text{Ce}_{0.8}\text{Y}_{0.2}\text{O}_{1.9}$ (YDC) powders calcined at $600\text{ }^\circ\text{C}$

about 50–60 nm and the particles were of spherical shape with good homogeneity and good dispersion.

The composite electrolyte ceramic was examined using SEM for microstructure. Figure 4 shows the SEM morphology of ceramic sample. It is seen that the surface layers of ceramic sample are made of a number of lamellae. This may be due to the fact that the phosphates in the $\text{YDC}-\text{Ca}_3(\text{PO}_4)_2-\text{K}_3\text{PO}_4$ composite melts at $1,400\text{ }^\circ\text{C}$ and spreads on the surface of the YDC particles, then solidifies as the process of temperature drops. In addition, some ball-shaped particles may be identified as the YDC particles [3, 5].

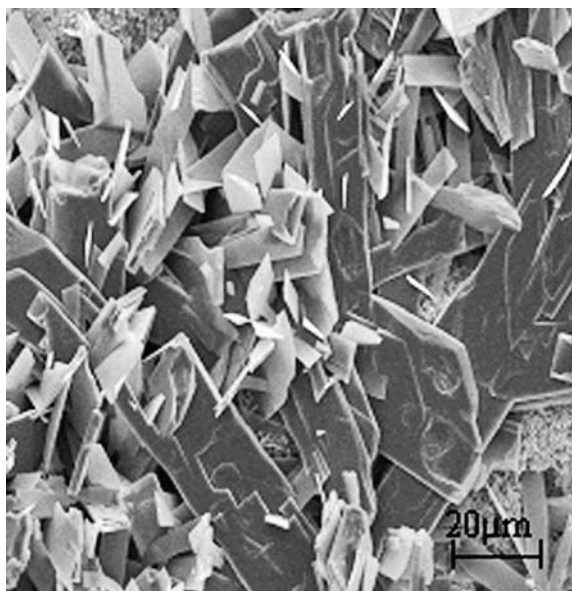


Fig. 4 SEM image of $\text{YDC}-\text{Ca}_3(\text{PO}_4)_2-\text{K}_3\text{PO}_4$ sintered at $1,400\text{ }^\circ\text{C}$

Electrochemical studies

In this paper, we investigated the ionic conductivity of the YDC and the YDC composite electrolytes in the temperature range $500\text{--}800\text{ }^\circ\text{C}$. Figure 5 shows temperature dependence of the conductivity of the YDC and the YDC composite electrolyte in natural gas/nitrogen. It is seen that the YDC composite electrolyte has demonstrated higher conductivity in comparison to the YDC electrolyte. At present, the detailed mechanism of the oxygen ion and proton conduction in this new composite material is still not clear, such as how the conductivity is enhanced once the two conducting solid phases are involved in the material, especially, the YDC already has a high defect concentration within its structure; what is the nature of the interfaces, thus the conducting mechanism, between the two conducting phases of the ceria and salts. All these and other related questions are still open [1].

Synthesis of ammonia at atmospheric pressure with the new composite electrolyte

First, the effect of potential on the rate of ammonia formation was tested at $650\text{ }^\circ\text{C}$. Figure 6 shows the results. It can be seen that the rate of ammonia formation increased by increasing the potential imposed on the cell, which confirmed that in the solid electrolyte cell reactors the ionic flux was not controlled by the hydrogen concentration gradient but rather by the imposed potential. We so can also see that the increasing tendency was swift at a lower potential and became gentle after 1.0 V. It was concluded in this paper that 1.0 V was the optimum potential for synthesizing ammonia.

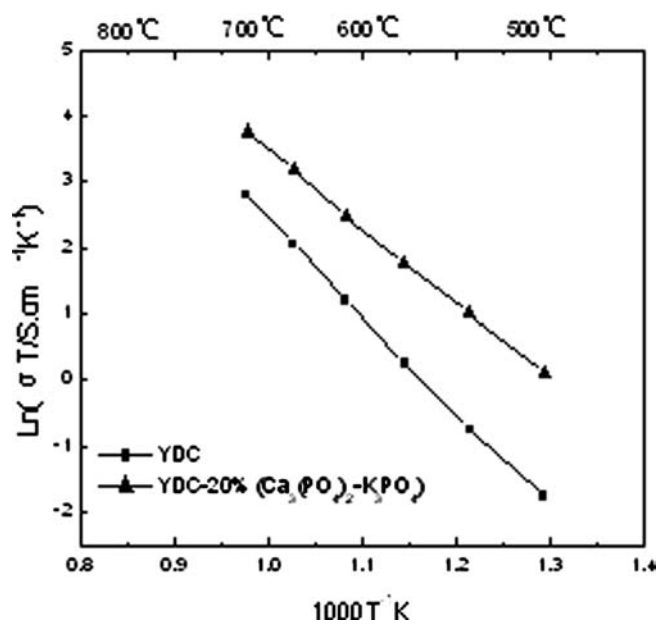


Fig. 5 Arrhenius plots of conductivity in YDC and $\text{YDC}-\text{Ca}_3(\text{PO}_4)_2-\text{K}_3\text{PO}_4$

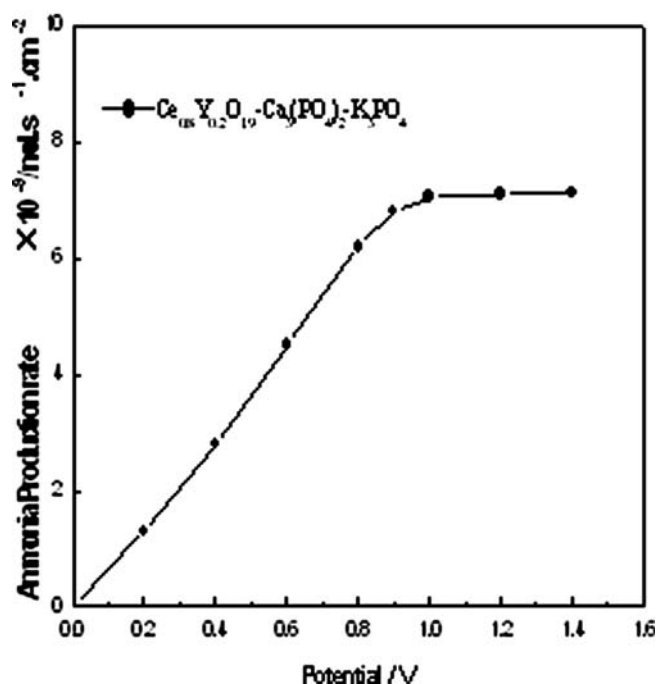


Fig. 6 Effect of the potential to the rate of NH_3 at 650 °C

Then, upon imposing a constant potential ($U = 1.0$ V) through the cell for a transient period of 10 min, when Nessler's reagent was added to the adsorption solution, a stable yellow color appeared immediately, which confirmed that NH_4^+ was present in the adsorption solution and had a reaction with the Nessler's reagent.

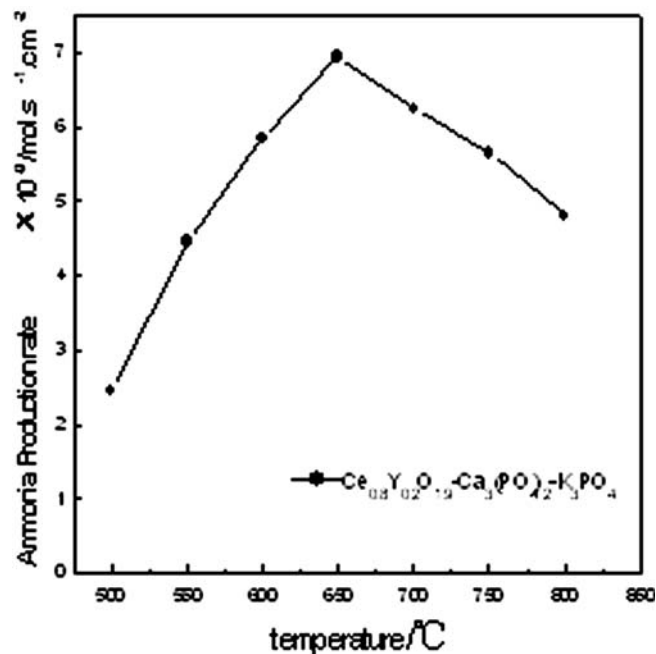


Fig. 7 Dependence of the ammonia production rate on the temperature

The concentration of NH_4^+ in the adsorption solution was measured at different operating temperatures by spectrophotometry. The rate of ammonia formation was calculated and was shown in Fig. 7. The rate of ammonia formation of the sample reached the maximum at 650 °C. Therefore, 650 °C was used as the optimum temperature in our experiments. This can be explained by the theory that the rate of ammonia formation depends not only on the capability of proton conduction and flow rate of natural gas and N_2 , but also on the rate of NH_3 decomposition [11]. Increasing temperature increases conductivity and at the same time, the rate of NH_3 decomposition also increases. This explains the peak in the curve of the rate of NH_3 formation as a function of temperature.

Although the chemical composition of natural gas varies according to the source, the principal component is methane, and the remainder is small amounts of low molecular weight hydrocarbons. Table 1 shows the compositions of natural gas used in our experiment.

Firstly, a depigmentation test was conducted by bubbling the tail gas. It was found that the tail gas can depigment Br_2 and KMnO_4 solution, which confirmed that alkene was present in the tail gas. At the same time, the hydrocarbon reaction products of the tail gas were analyzed using gas chromatography. Table 2 shows the results. According to the results, the possible mechanism of ammonia synthesis with the use of solid-state proton conductors from natural gas and nitrogen was explored. A model process that uses solid-state proton conductor from natural gas to generate hydrogen has previously been proposed [13–15]. According to the model process, the possible mechanism of ammonia synthesis is as follows:



Table 1 Gas chromatography analysis of natural gas

Component	Natural gas/%
CH_4	96.45672
C_2H_6	3.41842
C_3H_8	0.12504

Table 2 Gas chromatography analysis of the tail gas

Component	Tail gas/%
CH_4	95.59143
C_2H_6	3.71469
C_2H_4	0.18019
C_3H_8	0.51369

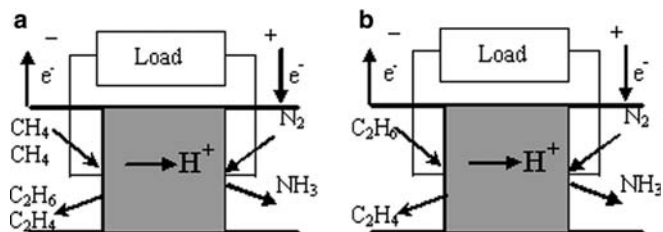


Fig. 8 Principle of the solid-state proton conducting cell reactor using YDC- $\text{Ca}_3(\text{PO}_4)_2$ - K_3PO_4 proton-conducting ceramic

Gaseous H_2 passing over the anode of the proton-conducting cell reactor will be converted to H^+ :



The protons (H^+) are transported through the solid electrolyte to the cathode where the half-cell reaction



takes place.

The principal schematic diagram of ammonia synthesis with the use of solid-state proton conductors from natural gas and nitrogen is as follows:

From Fig. 8, it can be seen that methane or ethane can be converted to hydrogen with the use of the YDC- $\text{Ca}_3(\text{PO}_4)_2$ - K_3PO_4 proton-conducting ceramic, and then ammonia was synthesized from nitrogen and hydrogen.

Conclusion

A new type of oxide-salt composite electrolyte, YDC- $\text{Ca}_3(\text{PO}_4)_2$ - K_3PO_4 , was developed and used as the electrolyte for the electrochemical synthesis of ammonia at intermediate temperature. This composite electrolyte exhibited much higher electrical conductivity than pure

YDC electrolyte, such that the composition of YDC and phosphates salts successfully improved the electrical conductivity at intermediate temperature range. Using this composite electrolyte, ammonia was synthesized from nitrogen and natural gas at atmospheric pressure. The rate of evolution of ammonia is up to $6.95 \times 10^{-9} \text{ mol s}^{-1} \text{ cm}^{-2}$.

Acknowledgements Work performed at Physical Electrochemistry Laboratory of Xinjiang University P.R.China is supported by Xinjiang P.R.China, Office of Science and Technology, Emphasis Project of Institution of Higher School, under fund project No. XJedu2004 I 11.

References

1. Bin Zhu (2003) *J Power Sources* 114:1
2. Zhu B, Yang XT, Xu J, Zhu ZG, Ji SJ, Sun MT, Sun JC (2003) *J Power Sources* 118:47
3. Zhu B, Liu X, Sun M, Ji S, Sun J (2003) *Solid State Sci* 5:1127
4. Zhu B, Liu X, Zhou P, Yang X, Zhu Z, Zhu W (2001) *Electrochem Commun* 3:566
5. Fu QX, Zha SW, Zhang W, Peng DK, Meng GY, Zhu B (2002) *J Power Sources* 104:73
6. Su XT, Liu RQ, Wang JD (2003) *Acta Chim Sinica* 4:505
7. Wang JD, Su XT, Liu RQ, HuY Xia, Xie YH, Yue F (2004) *Prog Chem* 5:829
8. Su XT, Liu RQ, HuY Xia, Xie YH, Wang JD (2004) *J Inorg Mater* 1:229
9. Xie YH, Wang JD, Liu RQ, Su XT, Sun ZP, Li ZJ (2004) *Solid State Ionics* 168:117
10. Xie YH, Liu RQ, Li ZJ, Wang JD, Su XT (2004) *Chin J Inorg Chem* 5:551
11. Marnellos G, Zisekas S, Stoukide M (2000) *J Catal* 193:80
12. Dicks AL (1996) *J Power Sources* 61:113
13. Iwahara H, Asakura Y, Katahira K, Tanaka M (2004) *Solid State Ionics* 168:299
14. Shenglu K, Wenfa X (1998) *Chem Eng Oil Gas* 3:144
15. Chiang PH, Eng D, Stoukides M (1993) *J Catal* 139:683
16. Shi YZ, Xiong XX, Chen XX (1998) *J Wuhan Metall Univ Sci Technol* 1:40